(13) Atalla, R. H. *Proceedings of International Symposium on Wood and Pulping Chemistry*; Tsukuba, 1983; Vol. 1, p 42.
(14) Atalla, R. H.; VanderHart, D. L. *Science* **1984**, *223*, 283.
(15) VanderHart, D. L.; Atalla, R. H. *Macromolecules* **1984**, *17*, 1465.
(16) Kunze, J.; Scheler, G.; Schroter, B.; Philipp, B. *Polym. Bull.* **1983**, *10*, 56.
(17) Fyfe, C. A.; Dudley, R. L.; Stephenson, P. J.; Deslandes, Y.; Hamer, G. K.; Marchessault, R. H. *J. Macromol. Sci., Rev. Macromol. Chem. Phys.* **1983**, *C23*, 187.
(18) Horii, F.; Hirai, A.; Kitamaru, R. *Polym. Bull.* **1983**, *10*, 357.
(19) Dudley, R. L.; Fyfe, C. A.; Stephenson, P. J.; Deslandes, Y.; Hamer, G. K.; Marchessault, R. H. *J. Am. Chem. Soc.* **1983**, *105*, 2469.
(20) Horii, F.; Hirai, A.; Kitamaru, R. In *Polymers for Fibers and Elastomers*; ACS Symposium Series 260 American Chemical Society: Washington, DC, 1984; p 27.
(21) Cael, J. J.; Kwoh, D. L. W.; Bhattacharjee, S. S.; Patt, S. L. *Macromolecules* **1985**, *18*, 821.
(22) Horii, F.; Hirai, A.; Kitamaru, R. *Macromolecules* **1986**, *19*, 930.
(23) Philipp, B.; Kunze, J.; Fink, H.-P. In *The Structures of Cellulose*; ACS Symposium Series 340; American Chemical Society: Washington, DC, 1987; p 178.
(24) VanderHart, D. L.; Atalla, R. H. In *The Structures of Cellulose*; ACS Symposium Series 340; American Chemical Society: Washington, DC, 1987; p 88.
(25) Barry, A.; Peterson, F. C.; King, A. J. *J. Am. Chem. Soc.* **1936**, *58*, 333.
(26) Yatsu, L. Y.; Calamari, T. A., Jr.; Benerito, R. R. *Textile Res. J.* **1986**, *56*, 419.
(27) Loeb, L.; Segal, L. *J. Polym. Sci.* **1954**, *14*, 121.
(28) Atalla, R. H.; Ellis, J. D. Schroeder, L. R. *J. Wood Chem. Technol.* **1984**, *4*, 465.
(29) TAPPI Standard Methods T230 om-82, 1982.
(30) Sihtola, H.; Kyrklund, B.; Laamanen, L.; Palenius, I. *Paperi ja puu* **1963**, *45*, 225.
(31) Henrissat, B.; Perez, S.; Tvaroska, I.; Winter, W. T. In *The Structures of Cellulose*; ACS Symposium Series 340; American Chemical Society: Washington, DC, 1987; p 38.
(32) Atalla, R. H. *Proceedings of the 4th International Symposium on Wood and Pulping Chemistry*; Paris, 1987; Vol. 1, p 215.
(33) Gomez, M. A.; Cozine, M. H.; Schilling, F. C.; Tonelli, A. E.; Bello, A.; Fatou, J. G. *Macromolecules* **1987**, *20*, 1761.

Growth of Polypropylene Particles in Heterogeneous Ziegler–Natta Polymerization

Masahiro Kakugo,* Hajime Sadatoshi, Jiro Sakai, and Masakazu Yokoyama

Sumitomo Chemical Co. Ltd., Chiba Research Laboratory, 5-1 Anesaki Kaigan, Ichihara, Chiba, 299-01, Japan. *Received April 4, 1988; Revised Manuscript Received November 4, 1988*

ABSTRACT: Nascent polypropylene particles prepared with δ-$TiCl_3$ catalyst systems have been examined by small-angle X-ray scattering, wide-angle X-ray diffraction, and electron microscopy. The catalyst crystallites which disperse at the initial stage of polymerization uniformly within the polymer particles retain their initial size during the course of polymerization. As the polymerization proceeds, the 0.2–0.35-μm primary polymer particles become visible under an electron microscope, and their size increases in proportion to the cube root of the polymer yield.

Introduction

In a previous paper we examined the architecture of nascent polypropylene particles prepared with heterogeneous Ziegler–Natta catalysts by transmission electron microscopy using a newly developed staining method.[1] The nascent polymer particles are made up of primary polymer particles which contain one or sometimes a few catalyst crystallites at the individual cores. The sizes of the catalyst crystallites within the primary polymer particles are in good agreement with that of the original catalyst crystallites. The primary polymer particles, 0.2–0.35 μm in diameter, are much smaller than the polymer globules observed on the surfaces of the nascent polymer particles, about 1 μm in diameter, which have so far been accepted as the primary polymer particles.[2] Such a difference in size suggests that several tens of the primary polymer particles probably constitute each of the polymer globules, i.e., secondary polymer particles. From these findings, we concluded that the nascent polymer particles may have a tertiary structure.

In olefin polymerization with the $TiCl_3$ catalysts it is observed in an electron microscope that the original catalyst particles disintegrate immediately into basic particles.[3,4] Hock reported that such basic particles retain their shapes during the course of polymerization.[3] On the other hand, Buls et al. reported that these basic particles break down further into smaller units.[4] Our previous observation of the nascent polymer particles indicated that the catalyst crystallites keep their initial shapes even at higher polymer yields.[1]

In the present work, we have examined the microstructure of the nascent polypropylene particles widely differing in polymer yield by using small-angle X-ray scattering (SAXS), wide-angle X-ray diffraction (WAXD), and electron microscopy to understand the growth mechanism of polymer particles during polymerization. From these observation we have concluded that the catalyst crystallites retain their sizes in the course of the polymerization and the primary polymer particles grow with the proceeding of polymerization.

Table I
Characteristics of Catalysts

catalyst	av particle size,[a] μm	crystallite size,[b] Å	polymerization activity,[e] g of polym/g of catal
δ-$TiCl_3$(I)	19	108,[c] 185[d]	1100
δ-$TiCl_3$(II)	18	75,[c] 75[d]	4500

[a] Determined by a sedimentograph with decaline as the disperse medium. [b] Determined with WAXD. [c] D_{300}, length of the primary catalyst crystallites normal to the (300) plane. [d] D_{003}, length of the primary catalyst crystallites normal to the (003) plane. [e] Polymerization was cararied out at 65 °C for 2 h in liquefied propylene.

0024-9297/89/2222-3172$01.50/0

Table II
Polymer Samples

sample	polymerization						
	catalyst	Ti/Al, mmol/L	temp, °C	press., kg/cm²	time, h	medium	yield, g/g[e]
A-1	δ-$TiCl_3$(I)	74/83[a]	65	1	1	heptane[b]	12
A-2		5.5/17[a]	60	26	0.5	propylene[c]	108
A-3		0.59/17[a]	60	26	4	propylene[c]	880
A-4		0.15/13[a]	65	29	5	propylene[d]	2030
B-1	δ-$TiCl_3$(II)	0.18/12[a]	60	11	1	heptane[d]	830
B-2		6.5/17[a]	60	26	1	propylene[c]	1400
B-3		0.06/13[a]	65	29	5	propylene[d]	8850

[a] $Al(C_2H_5)_2Cl$. [b-d] Polymerization was carried out (*b*) in a 0.2-L glass flask, (*c*) in a 0.1-L autoclave, and (*d*) in a 5-L autoclave. [e] Grams of polymer/gram of catalyst.

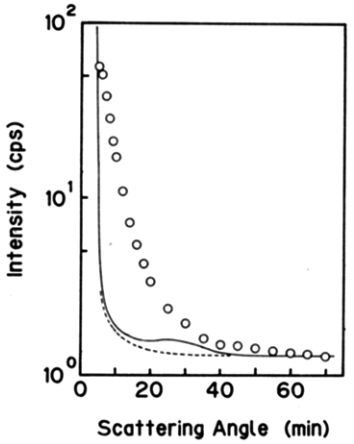

Figure 1. SAXS profiles of nascent polypropylene particles at the polymer yield of 12 g of polymer/g of catalyst (○) and of the polymer particles after removal of the catalysts (solid line). The dashed line is the scattering profile for an empty glass capillary.

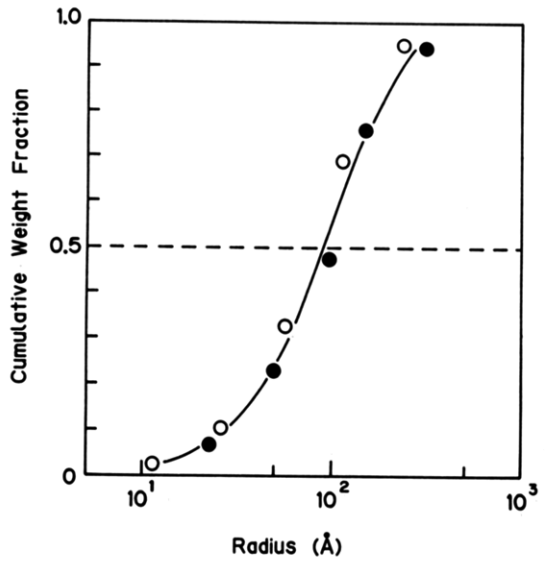

Figure 2. Particle size distributions obtained from the SAXS intensities of the δ-$TiCl_3$(I) (○) and the nascent polypropylene particles (●) prepared with the catalyst system.

Experimental Section

Catalyst. δ-$TiCl_3$(I) and -(II) were prepared by reduction of $TiCl_4$ with $Al(C_2H_5)_2Cl$ and treatment of the reduced products with diisoamyl ether and then with $TiCl_4$. The two forms of δ-$TiCl_3$ were slightly different in preparation conditions.

Polymerization. Polymerization was carried out in liquefied propylene or *n*-heptane. When the polymerization was carried out in liquefied propylene, the catalyst, hydrogen, and propylene were successively fed into a autoclave at room temperature and the polymerization was initiated by heating to the prescribed temperature. The polymerization was terminated by purging out propylene. In the solvent polymerization, *n*-heptane, the catalyst, hydrogen, and propylene were successively fed. The polymerization was terminated similarly by purging out propylene, and the polymer was filtered and dried.

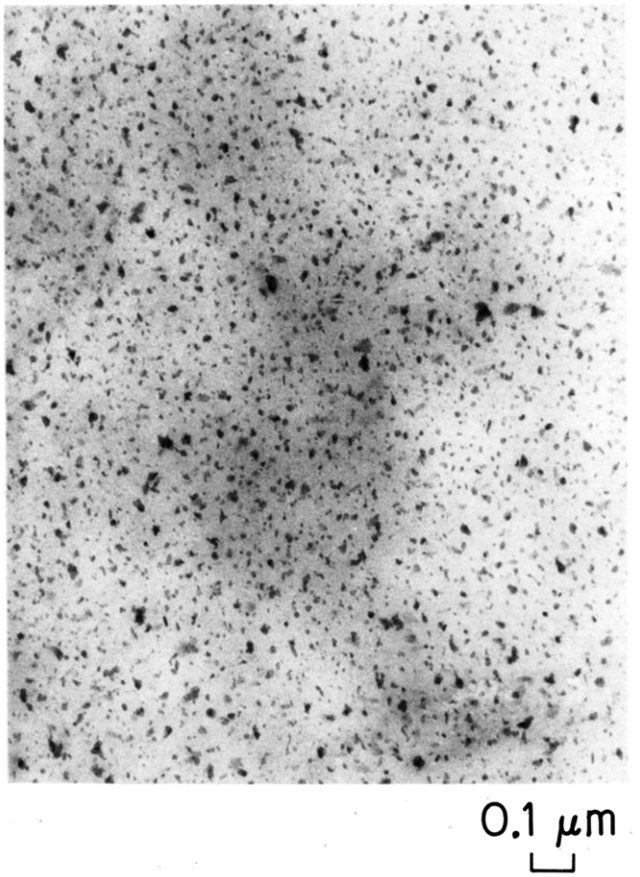

Figure 3. Transmission electron micrograph of the unstained section from a nascent polypropylene particle prepared with the δ-$TiCl_3$(I) catalyst system at the polymer yield of 12 g of polymer/g of catalyst. The specimen was not stained.

WAXD. WAXD measurement was carried out with a Shimadzu X-ray diffractometer VD-2, using a scintillation counter and a pulse height analyzer. Ni-filtered Cu Kα radiation was used. The crystallite size of δ-$TiCl_3$ crystallites was calculated from the line breadth of the diffraction peaks,[5] (003) at $2\theta = 15.0°$ and (300) at $2\theta = 51.5°$, by Scherrer's equation after correction had been conducted according to Warren's method.[7]

SAXS. Samples were examined in glass capillaries (1.0-mm diameter and 0.1-mm thickness) on a Simadzu X-ray diffractmeter VD-2 with Zr-filtered Mo Kα ($\lambda = 0.71$ nm). The collimating system was as follows. The second and third slits, the specimen, and the receiving slit were placed at 168, 273, 300, and 560 mm from the first slit, respectively. The sizes of the first, second, third, and receiving slits were 0.08 × 15, 0.06 × 15, 0.18 × 15, and 0.08 × 15 mm², respectively. The intensities were measured with a

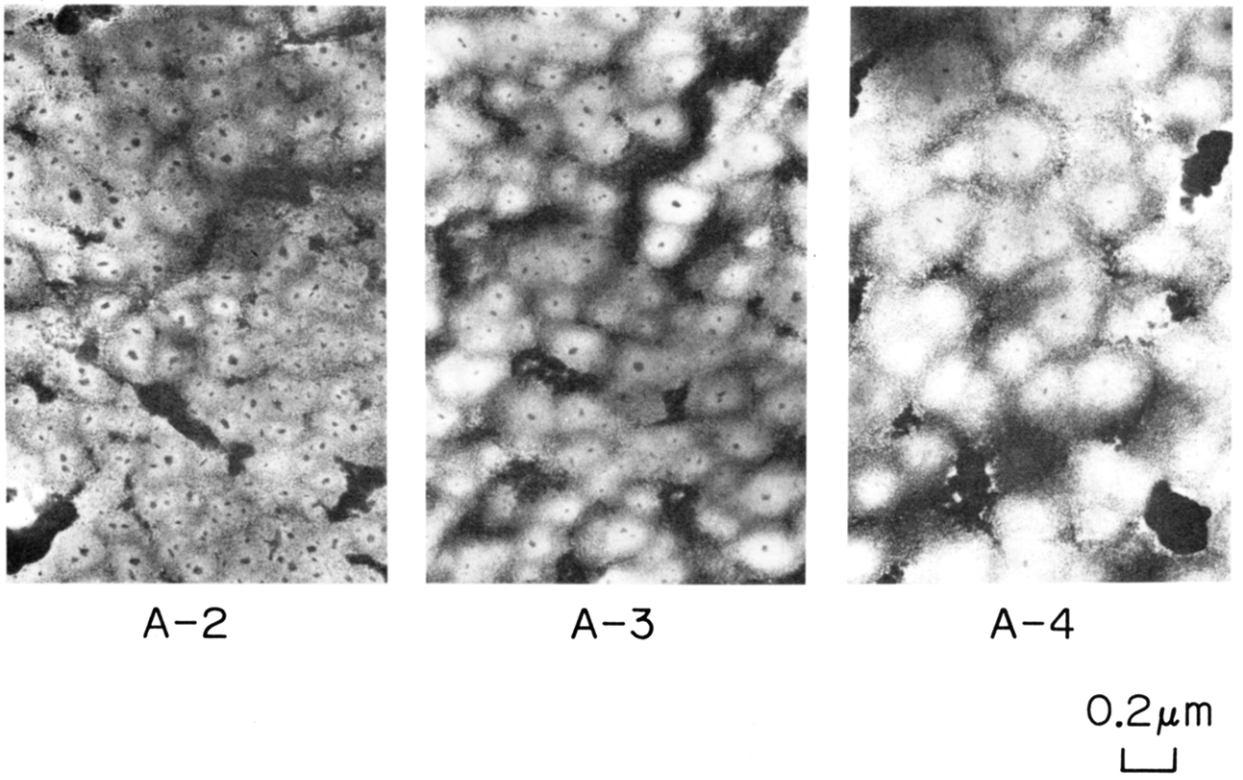

Figure 4. Transmission electron micrographs of polypropylene growth (catalyst, δ-$TiCl_3$(I)).

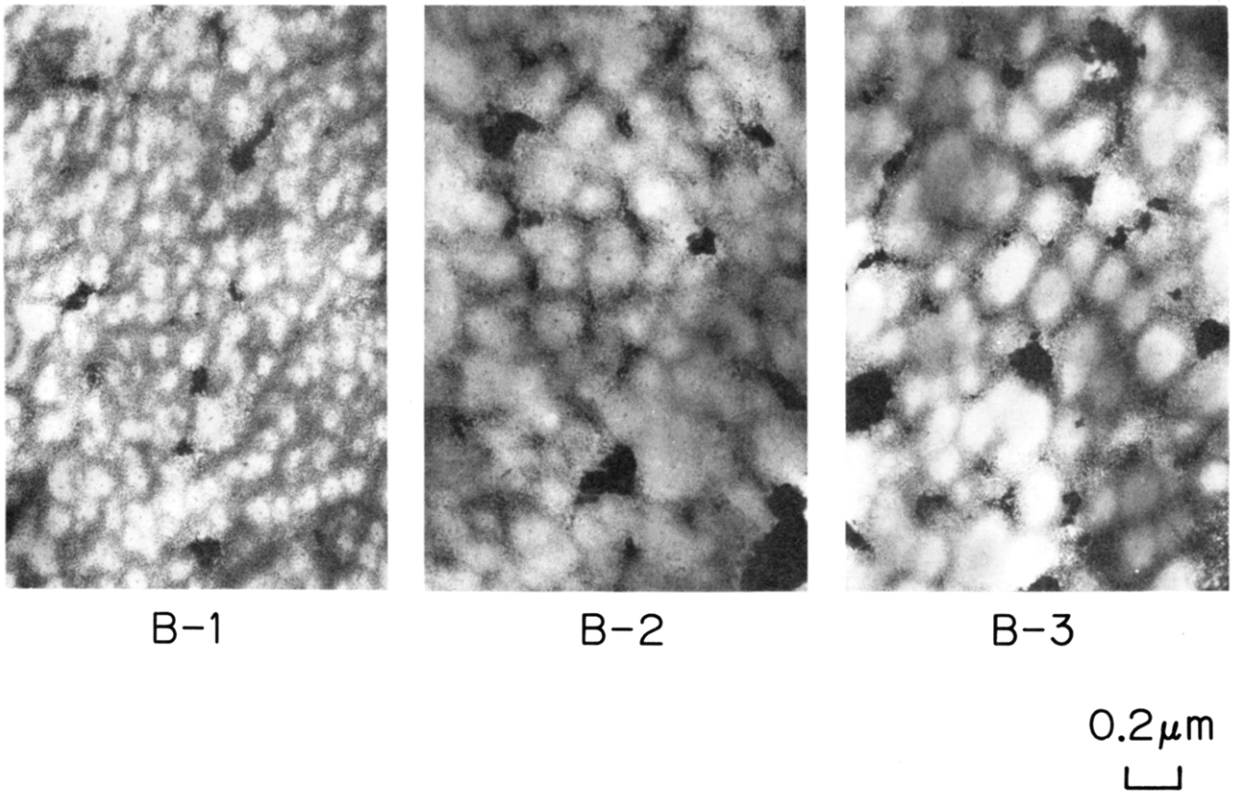

Figure 5. Transmission electron micrographs of polypropylene growth (catalyst, δ-$TiCl_3$(II)).

scintillation counter. The data were analyzed by Guinier-Fankuchen method corrected by Kakudo et al.:[8]

$$I = K\sum_{i=1}^{N} W_i \mathrm{Ro}_i^2 \exp(-4\pi^2/3\lambda^2\epsilon^2\mathrm{Ro}_i^2)$$

where I is the intensity, K a constant, λ the wavelength of the X-ray, ϵ the scattering angle, Ro_i the radius of the gyration of the ith particle, and W_i the weight fraction of the ith particle. When the particles are spheres with a radius of R, Ro is expressed by the following equation

$$\mathrm{Ro}^2 = (3/5)R^2$$

Electron Microscopy. The 1,7-octadiene/OsO_4 two-step staining procedure for transmission electron microscopic obser-

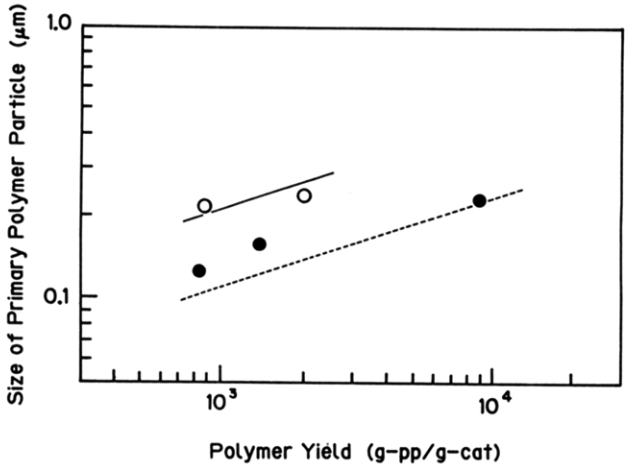

Figure 6. Relationship between the size of primary polymer particles and polymer yields in propylene polymerization: (○) δ-$TiCl_3$(I); (●) δ-$TiCl_3$(II). The solid line is the calculated relation for the δ-$TiCl_3$(I) catalyst system and the dashed line that for the δ-$TiCl_3$(II) catalyst system. The arithmetic mean of D_{300} and D_{003} was taken as the size of the catalyst crystallites.

vation was described previously.[1] Replication from some samples was carried out as follows. The sliced samples were etched with *n*-heptane at room temperature and replicated with cellulose acetate film. The replicas were prepared by a conventional two-stage method employing Pt–Pd and carbon. The procedure of scanning electron microscopic observation was described previously.[1]

Results and Discussion

The catalysts subjected to the present experiment are listed in Table I, where the average particle sizes, the dimensions of the catalyst crystallites, and the polymerization activities are shown. The polymer samples employed in this work are shown in Table II, where the polymerization conditions and the polymerization yields are described.

SAXS Measurement. First we examined the δ-$TiCl_3$(I) catalyst and the nascent polypropylene particles by using SAXS. Figure 1 shows SAXS intensity profiles for the nascent and purified samples of sample A-1 which was prepared with the δ-$TiCl_3$(I) catalyst system at the polymer yield of 12 g of polymer/g of catalyst. Sample A-1, after being purified, shows only a slight scattering peak near a scattering angle of 30 min which may be attributable to the primary polymer particles. On the other hand, the nascent sample A-1 shows strong scattering over the angle range 10–70 min, which results from the catalyst crystallites. The catalyst crystallite size distributions for sample A-1 and the δ-$TiCl_3$(I) catalyst were calculated[3] from the profiles after correction by backgrounds and scatterings from a glass capillary and the solid polymer. Figure 2 shows the resulting particle size distributions of the catalyst crystallites in sample A-1 and the original catalyst crystallites. Excellent agreement can be seen between them, which clearly shows that the catalyst crystallites did not break at least until the polymer yield exceeds 12 g of polymer/g of catalyst. The mean radius of the δ-$TiCl_3$(I) catalyst crystallites was found from the reading of the radius at 50% on the cumulative particle size distribution curve to be 180 Å. This value is very close to that determined by WAXD.

The nascent polypropylene, sample A-1, was examined by electron microscopy. Figure 3 shows a transmission electron micrograph of the nonstained specimen. One can see the dispersed particles, 100–200 Å in diameter, throughout polypropylene. In the preceding paper[1] we proved by X-ray microanalysis these particles to be the catalyst crystallites. The sizes of the catalyst crystallites observed in the electron microscope agree with the SAXS and WAXD data.

Electron Microscopic Observation. Figure 4 shows electron micrographs of samples A-2 through A-4 prepared with the δ-$TiCl_3$(I) catalyst system, varying in polymer yield. As the polymerization proceeds, polymer subparticles become visible. The particles contain some catalyst crystallites within each of them at intermediate polymer yield, i.e., 108 g of polymer/g of catalyst. As the polymer yield increases further, the number of the catalyst crystallites contained in the polymer subparticles decreases. At the polymer yield of 2030 g of polymer/g of catalyst, many polymer subparticles 0.2–0.35 μm in diameter con-

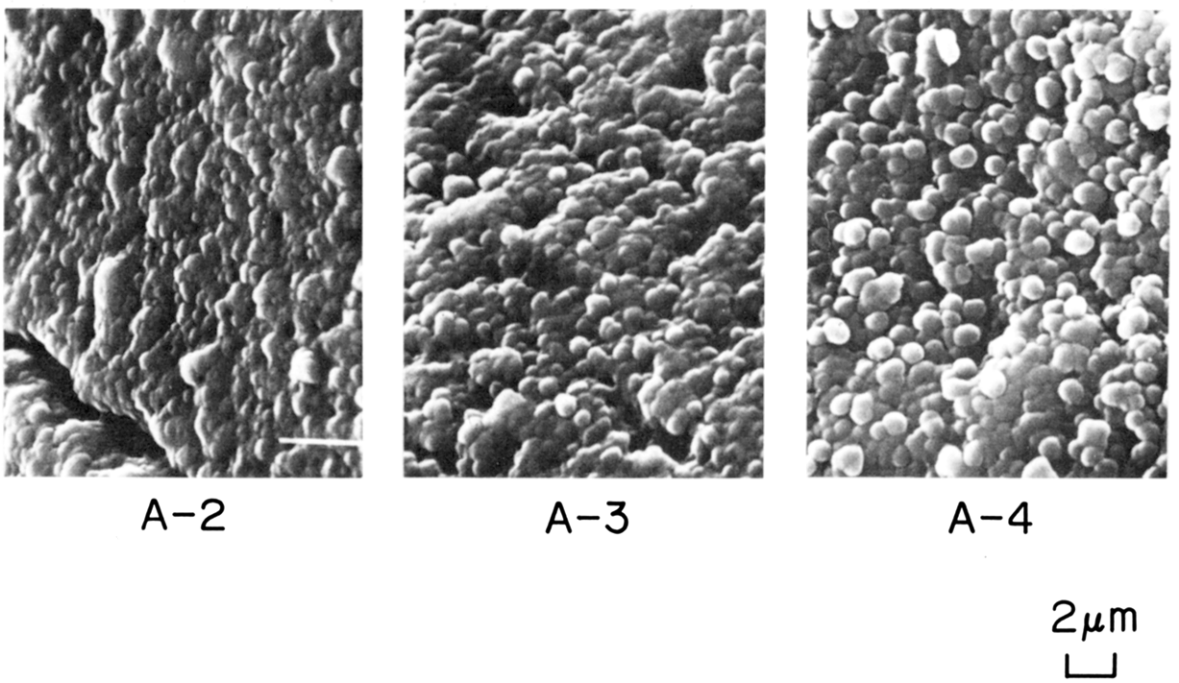

Figure 7. Scanning electron micrographs of polypropylene particles prepared with the δ-$TiCl_3$(I) catalyst system.

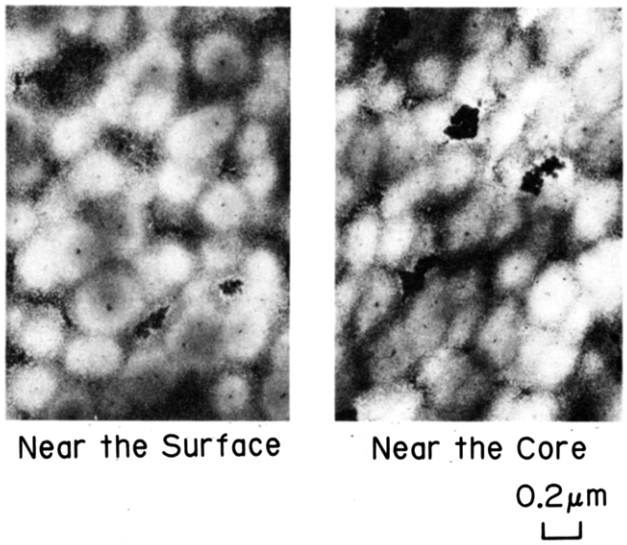

Figure 8. Transmission electron micrographs of the portions near the surface and core of a nascent polypropylene particle, sample A-4, prepared with the δ-$TiCl_3$(I) catalyst system.

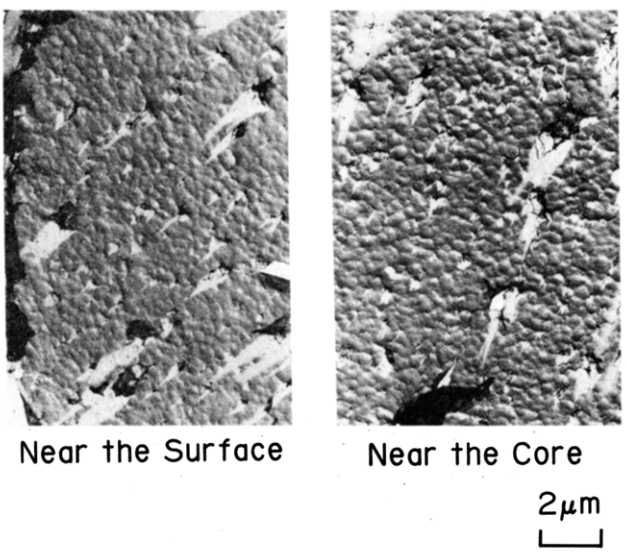

Figure 9. Transmission electron micrographs of the replicas from a nascent polypropylene particle, sample A-3, prepared with the δ-$TiCl_3$(I) catalyst system.

taining one catalyst crystallite near the center of them can be observed. At high polymer yield similar pictures were observed in the δ-$TiCl_3$(II) catalyst system, as shown in Figure 5. From these findings we have concluded the polymer subparticles containing a catalyst crystallite to be the primary polymer particles.

To make this point clearer, the average sizes of the primary polymer particles that contain a catalyst crystallite are plotted as a function of polymer yield on logarithmic graph paper in Figure 6. It has been generally accepted that the primary polymer particles grow surrounding the primary catalyst crystallite.[2,9] When this view is valid, an average diameter of the primary polymer particles (D) can be calculated from that of the catalyst crystallites (d) and the polymer yield (Y, grams of polymer/gram of catalyst) by the following equation:

$$D = d((\rho_{cat} Y/\rho_{pp}) + 1)^{1/3}$$

where ρ_{cat} is the density of the catalyst crystallite and ρ_{pp} that of polypropylene. A value of 2.7 g/cm^3 is taken as ρ_{cat} for $TiCl_3$ and 0.9 g/cm^3 as ρ_{pp}. The sizes of the primary polymer particles calculated from this equation are shown

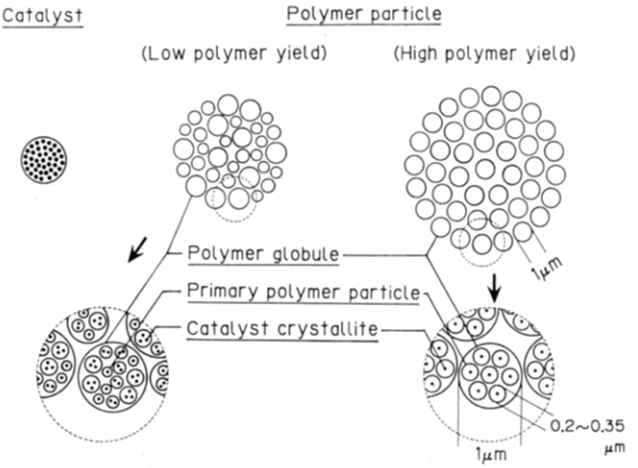

Figure 10. Schematic model for polypropylene growth.

together in Figure 6. The observed average sizes are close to those thus calculated. The δ-$TiCl_3$(II) catalyst gives small primary polymer particles compared with those from the δ-$TiCl_3$(I) catalyst at the same polymer yield, since the size of catalyst crystallites of the former catalyst are smaller.

Next, we examined the surfaces of these samples by scanning electron microscopy. Figure 7 shows electron micrographs of the polymer particles prepared with the δ-$TiCl_3$(I) catalyst system, varying in polymer yield. At low polymer yield equal to 108 g of polymer/g of catalyst, the polymer globules have a broad size distribution ranging from 0.4 to 1.1 μm. At a high polymer yield of 2030 g of polymer/g of catalyst, the polymer globules become round and uniform particles about 1 μm in diameter. These polymer globules are apparently much larger than the primary polymer particles observed in Figure 4. In the δ-$TiCl_3$(II) catalyst system a similar tendency could be observed. In order to understand how such polymer globules form, we observed the portions near the surface and the core of a polymer particle prepared with the δ-$TiCl_3$(I) catalyst system by transmission electron microscopy. Figure 8 shows micrographs of both portions. These pictures are almost identical and present no positive evidence supporting the presence of large polymer globules. Thus we examined the internal structure in the transmission electron microscope by using another method of sample preparation. A nascent polypropylene particle was sliced, etched with n-heptane, and replicated with cellulose acetate film. If each polymer globule consists of firmly bound primary polymer particles, one might expect that the polymer globules will be visualized by this method. Figure 9 shows transmission electron micrographs of the replicas near the surface and at the core of a polymer particle of sample A-3 prepared with the δ-$TiCl_3$(I) catalyst system. The two areas, which are almost identical, show an agglomerate structure of regular round particles ca. 0.5 μm in diameter. This size is close to that of the polymer globules 0.8 μm in diameter on the surfaces of the polymer particles observed by SEM. A slight difference between these sizes may be due to the difference in the sample preparation method. These sizes, however, are obviously larger than those of the primary polymer particles. This indicates that certain secondary structures are formed not only on the surface of the polymer particles but also in their interior.

In conclusion, a schematic model for polymer growth is illustrated in Figure 10. At the initial stage of polymerization the catalyst crystallites are dispersed uniformly

within the polymer particles. As the polymerization proceeds to a certain extent, the polymer subparticles containing some catalyst crystallites are formed. As the polymerization proceeds further, the polymer subparticles disintegrate to the primary polymer particles containing a catalyst crystallite, which grow as polymerization proceeds. The ca. 1-μm polymer globules on the surfaces of the polymer particles may be agglomerates of some tens of the primary polymer particles.

Registry No. $TiCl_3$, 7705-07-9; polypropylene, 9003-07-0.

References and Notes

(1) Kakugo, M.; Sadatoshi, H.; Yokoyama, M.; Kojima, K. *Macromolecules* **1989**, *22*, 547-551.
(2) Graff, R. J. L.; Kortleve, G.; Vonk, C. G. *J. Polym. Sci., Polym. Lett. Ed.* **1970**, *8*, 735-739.
(3) Hock, C. W. *J. Polym. Sci., Polym. Chem. Ed.* **1966**, *4*, 3055-3064.
(4) Buls, V. W.; Higgins, T. L. *J. Polym. Sci., Polym. Chem. Ed.* **1970**, *8*, 1037-1053.
(5) δ-$TiCl_3$ is shown by Guidetti et al.[6] to be the polymorphic of α- and γ-$TiCl_3$. In this study we describe the peak at 2θ = 51.5° as (300) as a matter of convenience, because α-$TiCl_3$ will be predominant in highly active δ-$TiCl_3$ as pointed out by Guidetti et al.[6]
(6) Guidetti, G.; Zannetti, R.; Ajo, D.; Marigo, A.; Vidali, M. *Eur. Polym. J.* **1980**, *16*, 1007-1015.
(7) Warren, B. E.; Biscoe, J. *J. Am. Ceram. Soc.* **1938**, *21*, 49-54.
(8) Kakudo, M.; Kasai, N.; Kimura, M.; Kubota, S.; Watase, T. *Nippon Kagaku Zasshi* **1957**, *78*, 821-825.
(9) Natta, G.; Pasguon, I.; Giachetti, E. *Chim. Ind. (Milan)* **1957**, *39*, 1002-1012.

Notes

Consideration of Hydrophobic Attractions in End-to-End Cyclization

KOOKHEON CHAR, CURTIS W. FRANK,* and ALICE P. GAST*

Department of Chemical Engineering, Stanford University, Stanford, California 94305-5025.

Received September 1, 1988;
Revised Manuscript Received November 30, 1988

Introduction

Cyclization of polymer chains has been of considerable interest for many years. It is related to fundamental problems such as synthesis of cyclic polymers and DNA cyclization[1] as well as practical problems such as physical property changes due to the addition of cyclic polymer to polymer blends. End-to-end cyclization has been investigated experimentally with the aid of spectroscopy. Sisido and Shimada[2] used the electron transfer between α-naphthyl or *N*-phthalimide groups attached to the ends of a polymer chain, monitored by electron spin resonance (ESR), to study the intramolecular end-to-end reaction. Luminescence techniques such as fluorescence and phosphorescence quenching have also been adopted[3] for polymer chains end-labeled with chromophores. These spectroscopic techniques use the common fact that when the two chromophores are in close proximity, these emit a band, for example, excimer emission, at a frequency distinguishable from the monomeric emission, thus permitting monitoring of the proximity of the ends. The end-to-end cyclization is generally dependent upon the conformation and the dynamics of the polymer chain connecting the two ends.[1,14]

End-to-end cyclization of polymers is known to be diffusion-controlled from extensive fluorescence studies,[1] implying that every encounter between chromophore ends leads to a dimer or excimer. Since the end-to-end cyclization is controlled by diffusion, the observed rate constant is proportional to T/η^0 where η_0 is the solvent viscosity and T is the absolute temperature. Recently, Cheung et al.[4] found anomalous behavior in the study of end-to-end cyclization using pyrene end-labeled poly(ethylene glycol) (Py-PEG-Py) in various solvents. They were able to correlate the measured excimer to monomer intensity ratio, I_e/I_m, which is proportional to the cyclization rate constant in the low-temperature limit, with the inverse solvent viscosity in all solvents except water and methanol where unusually high values of I_e/I_m were observed. Oyama et al.[5] also found similar anomalous behavior for Py-PEG-Py in water and further showed that the deviation of I_e/I_m in water from a diffusion-controlled process increases as the molecular weight of the PEG chain is decreased. In a previous paper,[6] we showed the effect of the addition of methanol on the viscosity-corrected excimer to monomer intensity ratio ($I_e(I_m\eta_0)$) for Py-PEG-Py in water. We found spectroscopic evidence for the existence of ground-state dimers in pure water and that the preformed dimers are diminished by the addition of methanol. From our experimental observations, we concluded that the ground-state dimers form in water-rich solvent due to the hydrophobic attraction between pyrene moieties.

Recently, this type of hydrophobically modified polymer chain has been used as an "associative thickener" in the paint industry.[7] Unlike conventional thickeners, which are usually nonadsorbing water soluble polymer, the associative thickeners interact with hydrophobic surfaces such as latex particles, improving the rheological properties of paint.[7]

The objective of this paper is to, first, derive a simple expression for the cyclization rate constant taking into account the hydrophobic attraction between pyrene ends and, second, to compare these predictions with the experimental results provided in our previous paper.[6]

Consideration of Hydrophobic Attraction

To derive a simple analytical expression, we consider a Gaussian polymer chain with negligible excluded volume. Since the Flory-Huggins interaction parameter (χ) for short PEG in water is close to $^1/_2$, the value representing the Θ condition, this approximation is reasonable. A general approach to model the hydrophobic attraction is to use a potential energy between hydrophobic moieties, such as a square-well potential, represented by both a depth (interaction energy) and a range of hydrophobic interaction. Since the interaction energy and the interaction range are generally coupled and there is no explicit expression for the hydrophobic attraction, we further wish to reduce a model potential to one adjustable parameter. There are two ways, in limiting cases, to reduce these two parameters into one. One approach leaves the interaction energy as the only parameter in a "sticky" potential[8] where the range of interaction is negligible. Another approach leaves the range of interaction as the adjustable parameter in a situation where the interaction is fairly high. Since the hydrophobic attraction is generally known to be long

0024-9297/89/2222-3177$01.50/0